

RESEARCH ARTICLE

OPEN ACCESS

## Capacitive Mosquito Wing-beat Sensor: A Novel Sensor for Intelligent Traps

Brendan Khoo T. T.\*, Muralindran M.\*\*, Rosalyn R. P.\*\*\*, W. W. Kitt\*\*\*\*

\*(Faculty of Engineering, Universiti Malaysia Sabah, Jalan UMS, 88400, Kota Kinabalu, Sabah, Malaysia

\*\* (Faculty of Engineering, Universiti Malaysia Sabah, Jalan UMS, 88400, Kota Kinabalu, Sabah, Malaysia

\*\*\* (Faculty of Engineering, Universiti Malaysia Sabah, Jalan UMS, 88400, Kota Kinabalu, Sabah, Malaysia

\*\*\*\* (Department of Electrical and Computer Engineering, Curtin University, Miri Sarawak, Malaysia

### ABSTRACT

Despite the vast advancement in science and modern technology, disease carrying mosquitoes are still hard to control and have caused damages, sufferings and deaths around the globe. In recent years, many research efforts have been put into the automation of insect species recognition to improve mosquito surveillance efficiency. These works commonly utilize the wing-beat or wing-flap characteristics obtained from optical or acoustic sensors to accurately predict the species or type of insect via modern classification techniques. However, instead of conventional acoustic or optical based sensor, this paper demonstrates a novel capacitive sensor for sensing mosquito wing-beat. The proposed sensor uses the electrocuting grids of an insect zapper as the sensing elements for detecting mosquito wing-beat. This sensing method opens a new possibility in utilizing electrocuting grid to selectively kill insects of a specific species or type. This paper highlights the initial design of this sensor and its performance with live mosquito samples.

**Keywords** - Capacitive Sensor, Insect Species Recognition, Insect Surveillance, Insect Trap, Intelligent Trap, Smart Trap, Wing-beat Sensor

Date of Submission: 18-07-2020

Date of Acceptance: 02-08-2020

### I. INTRODUCTION

Insects like many other living organisms play an important role in our health, social and economy. The presence of insects can be either beneficial or harmful depending on their species and role in the ecosystem. Insects like *Anopheles*, *Aedes* and *Culex* mosquitoes are notoriously known as vectors for highly damaging diseases (Malaria, Dengue fever, Yellow fever, Zika fever, Chikungunya and etc.). In 2017 alone, there were 219 million cases of malaria worldwide and 435,000 of them had resulted in deaths [1]. Besides affecting the health of the citizen, the plight caused by these mosquitoes could undermine the economy by destroying the tourism industry, livestock and the confidence of the business investors [2]. This has spurred many dedicated interdisciplinary researches to control, survey and also to better understand these pests.

In the recent decade, many sensors and algorithms were proposed for insect species recognition that could help in insect surveillance and monitoring efforts. These sensors are incorporated into modified insect traps [3] to make the collection and counting of insects automatic. Conventionally, these procedures are manually processed with

adhesive or suction traps that are placed and collected periodically for analysis by trained field workers. These samples will then be brought to a laboratory for manual sorting and counting under a microscope by taxonomists [4], consequently very expensive and time consuming.

Recently, many works on automated species recognition for flying insects center on wing-beat sensing. These works commonly utilize a microphone [5], [6] or an optical sensor [7]–[10] to capture the wing-beat signal of the flying insect, however, the optical counterpart has gained higher prominence due to better noise performance. Although the initial concept of optical insect wing-beat sensor used a photoelectric cell with sunlight as light-source [11], recent sensors are based on photodiodes and phototransistors with lasers [7], [12], [13] or LEDs [10], [14], [15] as light-source. Optical insect wing-beat sensors were tested with different algorithms for species recognition: Dynamic Time Warping-Delta (DTW-D) [16], Bayesian [17], Dynamic Time Warping (DTW) with nonlinear median filtering (NMF) [18], Mel-Frequency Cepstral Coefficients (MFCC) with SVM-RBF [19], robust stacked autoencoder (R-SAE) with SVM [20] and kernel adaptive autoregressive-moving average (KAARMA) [12].

The advancement in both insect wing-beat sensing and species recognition has also moved the concept of selective trapping or capturing closer to reality. Selective trapping can be described as an ability to capture or kill insects of a target species while not harming insects of other species. This type of trap can prevent sample contamination and unintentional destruction of beneficial insects. A paper by Silva et al. [19] has briefly described a mechanical actuated smart trap that lures mosquitoes via a selected attractant (example: carbon dioxide) and pull them into the trap via suction airflow. Inside the trap, a laser wing beat sensor is placed before an actuated door to detect the species of the attracted insect. If the target insect species is detected, the actuated door will allow the insect into the trapping chamber where the insect will be adhered to a sticky paper. A more detailed design of such technology is elaborated in [21], where, multiple cells with individual automated doors and sensors are arranged in a maize-shaped configuration. Each of these automated doors are actuated with an electromagnetic or electrical mechanism.

In this paper, a novel capacitive wing-beat sensor is proposed as a potential alternative to conventional optical wing-beat sensor. As the name suggests, it measures the small capacitive changes induced by the wing-beat of a nearby insect. This novel sensor can be easily integrated into conventional electrocuting traps by using the existing electrocuting grids as the capacitive sensing electrodes. This concept could provide a simple but significant upgrade to current commercial electrocuting traps and could potentially replace conventional suction or adhesive traps in surveillance applications [22], [23]. As opposed to optical wing-beat sensors, the proposed method could have better durability in harsh environment and lesser maintenance as it does not involve sensitive optical components such as laser diodes, optical lenses and photodiodes. Besides that, an intelligent trap derived from this sensing method will require no additional sensor elements and no moving mechanical parts that will cause significantly higher manufacturing and designing costs, additional mechanical wear, and larger size when compared to its non-intelligent counterpart. This low barrier-of-entry and simple operation can motivate and muster cooperative efforts from all members of the society to maintain, fund and operate the intelligent traps independently instead of limiting the application to only experts and large organizations.

## II. INTELLIGENT MOSQUITO TRAP

The proposed concept for converting current commercial insect zapper into an intelligent mosquito trap has a very simple setup. It consists of a capacitive sensor module, embedded processor, high voltage relay and wireless internet module (cellular or Wi-Fi). As shown in Fig. 1, the capacitive sensor module is connected directly to the electrocuting grid of the commercial insect trap via a high voltage relay, and actively measuring the capacitance change in the surrounding of the grid. The analog signal output of the capacitive sensor module is then fed into an ADC connected to the embedded processor. The embedded processor computes the capacitive signal and makes the decision (according to the insect species obtained from wing-beat information) to either ignore or energize the coil of the high voltage relay. When energized the relay will switch the connection of the electrocuting grid from the capacitive sensor module to the high-voltage supply. The count of the electrocuted mosquito will be transmitted to the central server through wireless internet connection for population analysis.

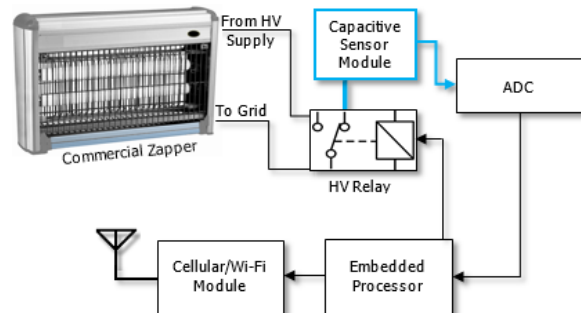


**Fig. 1. The proposed concept**

Fig. 1 shows the overall layout of the proposed system. However, the scope of this paper will only cover the design of the capacitive sensor module used for measuring the capacitive change caused by insect wing-beat. The following sections will discuss the construction of the sensing grid, capacitive sensing circuit and the chamber for signal acquisition and testing.

## III. CAPACITIVE WING-BEAT SENSOR

The operation of a capacitive sensor usually involves charging up conductive electrodes and discharging them periodically to measure the amount of charge stored. The amount of electrical charge stored in the electrode is influenced by the nearby conductive surface and also the dielectric characteristic of the medium. Capacitance,  $C$  is influenced by the permittivity of the medium,  $\epsilon$ , surface area of the electrode,  $A$ , and distance to the

second electrode or a nearby conductive surface, d, in the form of equation (1).

$$C = \frac{\epsilon A}{d} \quad (1)$$

Capacitive sensors generally operate in three modes, loading mode, shunt mode and transmit mode [24]. In the loading mode, the sensor has a single electrode projecting electric field that interacts with nearby grounded conductive object, producing different resultant capacitance. Shunt mode uses two electrodes, transmit and receive. The transmit electrode actively powers the electric field between itself and the receive electrode, hence, when a grounded conductive object approaches, part of the projected field will be grounded, reducing the measured capacitance at the receiving electrode. The transmit mode operates differently from shunt mode although both of them have transmit and receive electrodes. Transmit mode uses the nearby conductive object to extends the electric field to the receive electrode, thus increasing the measured capacitance. Fig. 2, illustrates the three common modes of capacitive sensing. The capacitive sensor in this paper is required to measure the capacitive change caused by mosquito wing movement when airborne (mosquito not conducting to ground/completing the electrical loop), therefore, transmit mode is the most suitable for this application.

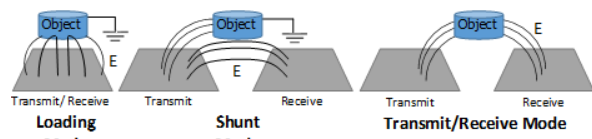


Fig. 2. Common capacitive sensing modes

The capacitive sensor module proposed in this paper has six functional stages: transmit electrode, receive electrode, high-frequency sinusoidal voltage source, preamplifier, tuner, AM demodulator and band-pass amplifier. The sensing grid has alternating transmit and receive conductive rods acting as capacitive sensing electrodes. The high-frequency sinusoidal voltage source is connected to the transmit electrodes to excite the electrodes with fixed frequency and amplitude, as excitation source for capacitance measurement. The excitation signal coupled across the transmit and receive electrodes is buffered by the preamplifier stage to preserve the signal quality and prevent attenuation by the input of the tuner stage. The tuner stage removes all the out-of-band noise and signal with a narrow band-pass filter. At the AM demodulator stage, the filtered signal from tuner stage is amplitude demodulated to obtain the capacitance change influenced by insect wing-beat across the receive and transmit electrodes.

The demodulated signal is then band-pass filtered and amplified to cover only the wing-beat frequencies and the harmonics of most common mosquitoes (150Hz – 2000Hz) in band-pass amplifier stage. This stage prepares the signal for digitization or further processing by removing ambient noise and the remaining carrier component while amplifying the useful frequency spectrum to the optimum amplitude. Fig. 3 illustrates the overall flow of the stages mentioned.

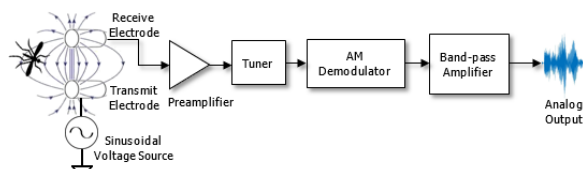


Fig. 3. The functional flow of the proposed capacitive sensor

### 3.1 Excitation Source and Sensing Electrodes

At the transmission side, the excitation source is a waveform generator, supplying an AC voltage to the transmit electrodes. The waveform generator used in this paper can be replaced with a low-noise crystal oscillator circuit when implemented in the actual sensor. The transmit and receive electrodes used in this paper are 1.8 mm stainless steel rods. The electrodes are secured with two High-Density Polyethylene (HDPE) brackets at both ends and are spaced equally at 8 mm apart. As shown in Fig. 4, the transmit and receive electrodes are positioned alternately and connected in parallel with connector blocks.

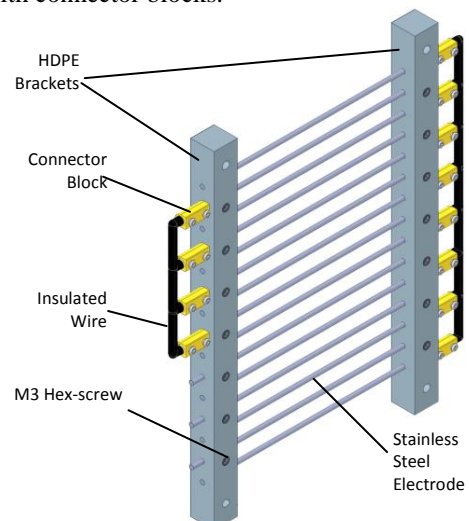


Fig. 4. Electrocutting grids (sensing electrodes) grids (sensing electrodes)

### 3.2 Preamplifier Stage

The preamplifier stage consists of a non-inverting low noise amplifier (LNA) circuit. The

amplifier IC for this circuit is an AD8066, a dual channel version of the AD8065 FET op-amp. This amplifier is selected specifically for its low input noise ( $7\text{nV}/\sqrt{\text{Hz}}$  and  $0.6\text{ fA}/\sqrt{\text{Hz}}$ ), low input bias current ( $1\text{ pA}$ ), high slew rate ( $180\text{ V}/\mu\text{s}$ ), low input capacitance, high band-width ( $42\text{MHz} @ 2\text{VPP}$ ) and low distortion specifications. Shown in Fig. 5, is the preamplifier circuit operating on dual-supply ( $\pm 5$ ).

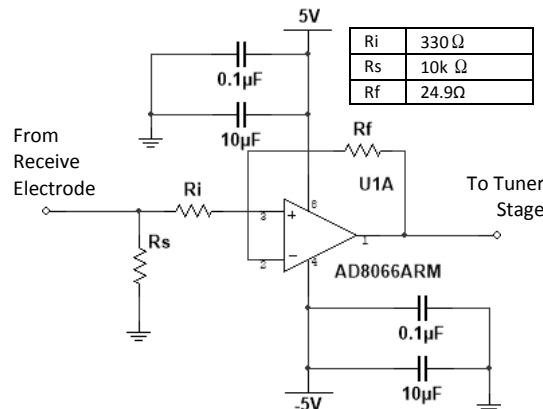


Fig. 5. Preamplifier circuit

### 3.3 Tuner Stage

The main purpose of the tuner stage is to filter out all the out-of-band noise and signal that have been picked up and propagated from prior stages. This stage is primarily a narrow band-pass filter tuned to the carrier frequency of the sensor excitation source. This filter is implemented conveniently on an active-RC-filter IC, LT1568, using six passive components. The LT1568 can be easily configured to perform as either a low-pass, a high-pass or a band-pass filter with changes to its peripheral components. Each IC has two 2<sup>nd</sup>-order filter-building-blocks that are accurately trimmed and matched. Displayed in Fig. 6 are two 2<sup>nd</sup> order band-pass filter block connected in series in the tuner stage.

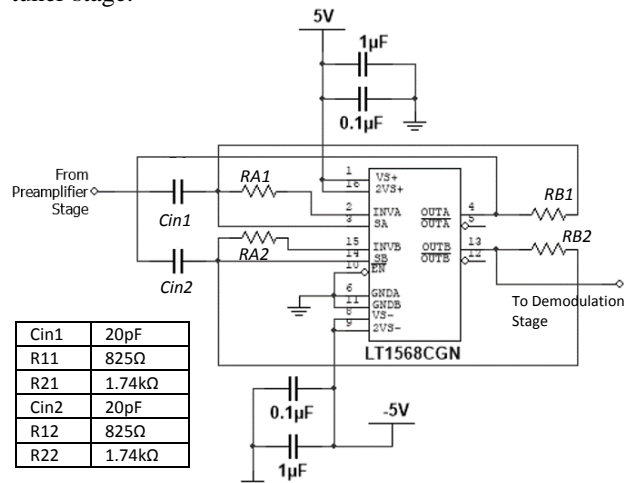


Fig. 6. The tuner stage circuit

The characteristics of the band-pass filter blocks can be manipulated individually with the peripheral components,  $R_A$ ,  $R_B$ , and  $C_{in}$ . The transfer function for each filter block can be represented as equation (2).  $C_{1A}$  and  $C_{2A}$  are the internal trimmed capacitors valued approximately  $105.7\text{pF}$  and  $141.3\text{pF}$  respectively.

$$-\frac{V_o}{V_i} = \frac{\frac{C_{in}R_B}{s C_{1A}R_A R_B(C_{2A} + C_{in})}}{s^2 + s \frac{C_{1A}(R_A + R_B) - C_{2A}R_B}{C_{1A}R_A R_B(C_{2A} + C_{in})} + \frac{1}{C_{1A}R_A R_B(C_{2A} + C_{in})}} \quad (2)$$

The center frequency,  $f_0$ , quality factor of the single band-pass stage,  $Q$ , and the gain of the filter block,  $H$ , are estimated in equations (3), (4) and (5).

$$f_0 = \frac{1}{2\pi} \sqrt{\frac{1}{C_{1A}R_A R_B(C_{2A} + C_{in})}} \quad (3)$$

$$Q = \frac{\sqrt{C_{1A}R_A R_B(C_{2A} + C_{in})}}{C_{1A}(R_A + R_B) - C_{2A}R_B} \quad (4)$$

$$H = \frac{C_{in}R_{21}\sqrt{C_{1A}R_A R_B(C_{2A} + C_{in})}}{(C_{1A}(R_A + R_B) - C_{2A}R_B)^2} \quad (5)$$

### 3.4 Demodulation Stage

At the demodulator stage, the output from the tuner stage is used to drive an envelope detector circuit. This circuit tracks the amplitude of the carrier/excitation signal. Any capacitance fluctuation, in this case, the capacitance change caused by an airborne insect flapping its wings will be registered by this circuit. Shown in Fig. 7, the wing-beat signal in the form of varying capacitance is obtained as the voltage across  $R_dC_d$ . This signal is buffered with the remaining amplifier channel in AD8066 before inputting into the band-pass amplifier stage. The peak-detector diode  $D_1$  in Fig. 7 is 1N5711 UHF/VHF Schottky diode.

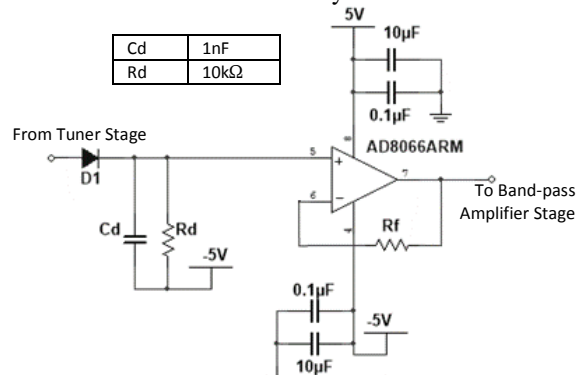


Fig. 7. Envelop detector circuit for the demodulation stage

The values for  $C_d$  and  $R_d$  can be estimated via equation (6), where  $m$  is the modulation index and  $\omega_b$  is the frequency of the insect wing-beat signal [25].

$$\frac{1}{R_d C_d} \geq m\omega_b \quad (6)$$

### 3.5 Band-Pass Amplifier Stage

The band-pass amplifier stage prepares the capacitive wing-beat signal obtained from the demodulation stage for output or further processing. The raw-wing-beat signal extracted using the envelop detector in prior stage is extremely faint and contains out-of-band noise, hence, must be band-pass filtered and also amplified to a useful level first before outputting. This is done using an 8<sup>th</sup>-order active-band-pass filter circuit tuned to include common mosquito wing-beat frequencies and harmonics. This circuit comprises of two Multiple-feedback-low-pass and two Sallen-Key-high-pass filters in tandem as shown in Fig. 8.

R1A	12.4kΩ	R1C	21kΩ
C1A	100nF	C1C	100nF
C2A	100nF	C2C	100nF
R2A	8.45kΩ	R2C	3.24kΩ
R3A	6.81kΩ	R3C	8.87kΩ
R4A	3.09kΩ	R4C	1.02kΩ
C1B	100nF	C1D	100nF
R1B	3.74kΩ	R1D	1.3kΩ
R3B	2.87kΩ	R3D	12.4kΩ
R2B	12.1kΩ	R2D	1.18kΩ
C2B	2nF	C2D	6.8nF

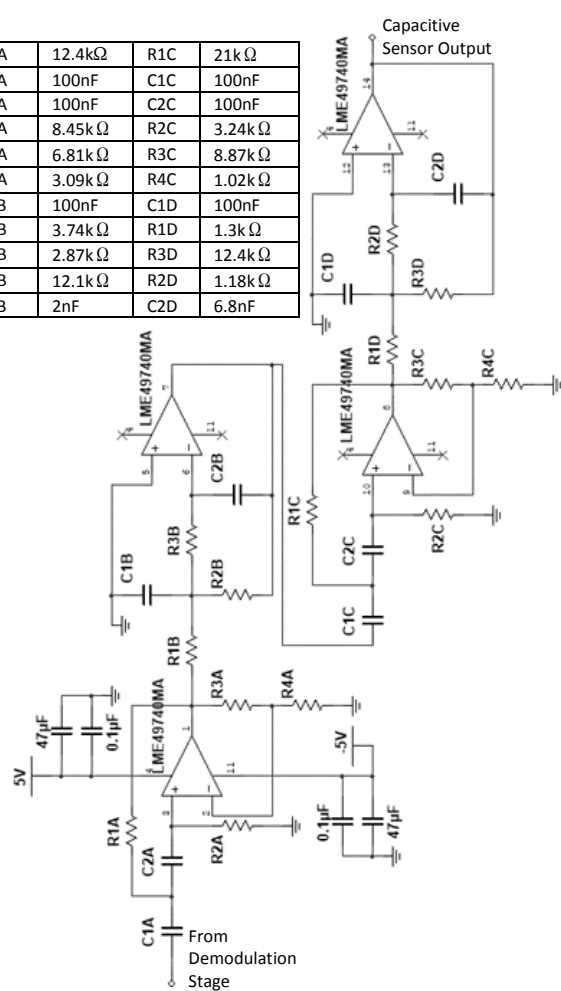


Fig. 8. Band-pass amplifier stage

These filter stages are implemented on a single quad-amplifier IC, LME49740. LME49740 is a high-fidelity audio operation amplifier with very low input noise density (2.7nV/√Hz at 1kHz), very high GBW product (55 MHz minimum), very low distortion (THD+N = 0.00003%), high common mode rejection ration (CMRR = 120dB), high power supply rejection ration (PSRR = 120dB), high open

loop gain (140dB when loaded with 600Ω) and low input bias current (10nA).

The active high-pass-filter stages are configured to provide a 4th-order Chebyshev 0.01dB response with 150Hz passband (-3dB) and 50Hz stopband (-40dB) to block any residual mains noise from reaching the final output. As for the active low-pass-filter stages, they are set to 4th-order Chebyshev 0.01dB response with 2kHz passband and 5.6kHz stopband to remove all high-frequency noises above common mosquito wing-beat frequencies [26]. The faint insect wing-beat signal is also amplified to approximately 961V/V (59.65dB) to increase the signal amplitude to a measurable level for recording/measuring instrument, which, in this paper is an oscilloscope. This is achieved by adjusting the gain for both high-pass and low-pass stages of this circuit to around 31 V/V (29.83 dB) respectively.

## IV. EXPERIMENT

### 4.1 Test Chamber

The test chamber is a custom tool catered for this research to maintain a controlled environment for testing the proposed mosquito wing-beat sensor. It is designed to provide a flexible and convenient way to insert insect samples into a confined chamber where the test sample is able to fly and interact with the sensing electrodes (electrocutting grids) freely. It comprises of two mirror halves of laser-cut transparent acrylic parts as shown in Fig. 9. The halves are held together with four screws and nuts, clamping lightly on the stainless-steel electrodes, over thin layers of polyethylene foam/sponge (to provide mechanical damping and stress relieve) as in Fig. 10. At both ends of the chamber, sample insertion entrances are made to conveniently transfer insect samples held in a laboratory/medical plastic container into the chamber. In order to assist the sampling and signal acquisition process of the test chamber, optical fiber sensors are used to sense the crossing of the flying insect near the grids.

The optical fibers (emitter and receivers) of each object sensor are placed on the opposite site of the chamber to create a “sensing curtain” that triggers when the insect crosses the line-of-sight of the optical fiber. There are two “sensing curtains” at opposite sides of the sensing electrodes (Fig. 11). This additional sensing setup can provide a reference or a trigger mechanism in an automated signal acquisition, in this case, a trigger source for the oscilloscope to single shot capture the insect wing-beat waveform without any manual intervention. The optical object sensors employed in this research are Panasonic FX-300 and Keyence FS-V31.

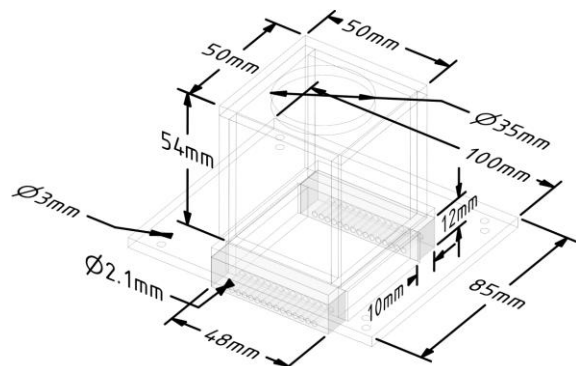


Fig. 9. An acrylic assembly half of the test chamber

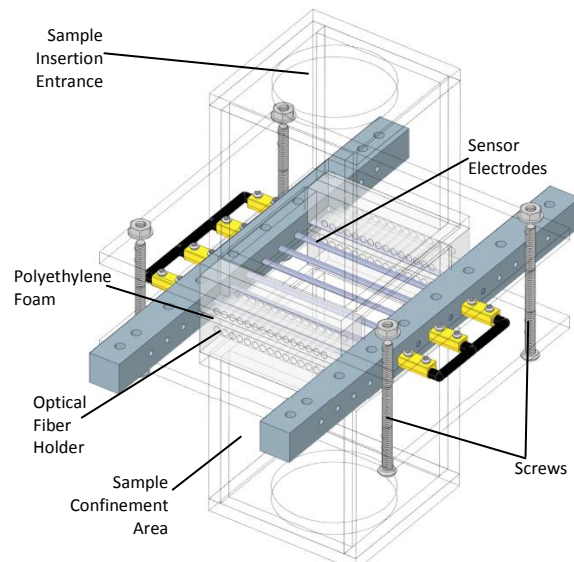


Fig. 10. Test chamber with sensor electrodes mounted

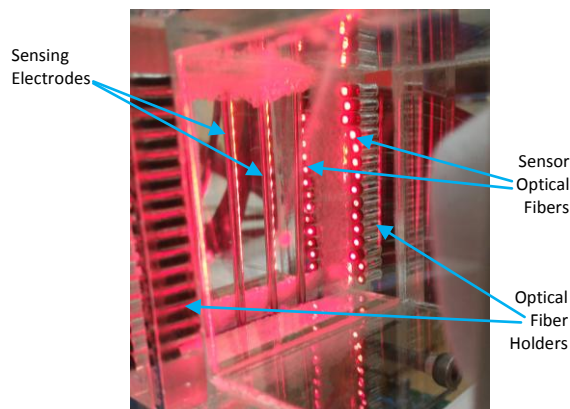


Fig. 11. The optical fibers secured at the holders around the sensing electrodes

#### 4.2 Sensor Circuit

The proposed capacitive wing-beat sensor circuit is developed on a dual layer PCB. However,

this test circuit is implemented with circular-hole sockets (to connect with through-hole components) in place of discrete passive and active components that determine the core parameters of the sensing circuit. This design offers flexibility and modifiability to the test circuit. The final populated test circuit is as shown in Fig. 12.

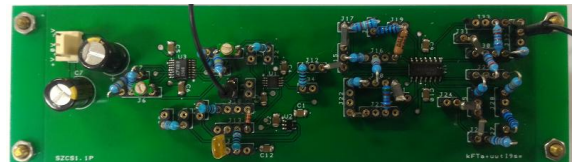


Fig. 12. The test circuit for the proposed sensor

#### 4.2 Experimental Setup

The experimental setup used for testing the proposed sensor is comprised of a waveform generator as the sensor excitation source, dual-channel digital oscilloscope as output recording instrument, 30 optical object sensors, the test chamber and the capacitive wing-beat sensor circuit. As illustrated in Fig. 13, the sensor excitation source (Agilent 33500B waveform generator) supplies a 1MHz sinusoidal voltage signal at  $5V_{peak}$  amplitude to the transmit electrodes in the test chamber.

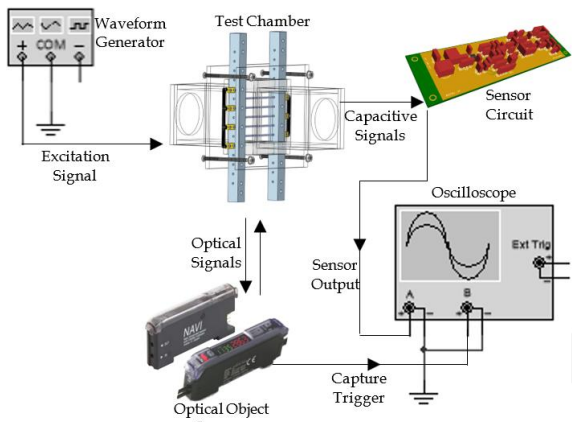
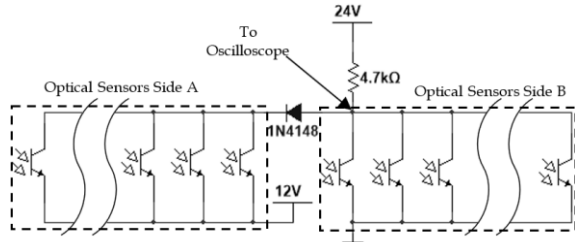


Fig. 13. Overview of the experimental setup

The connection of the receive electrodes to the input of the preamplifier circuit must be kept as short as possible to reduce parasitic capacitance as well as external noise. The output of the capacitive wing-beat sensor circuit is fed into a digital oscilloscope (Tektronix DPO2012) for recording. As for the optical object sensors, they are setup accordingly to Fig. 14. All the open-collector outputs of the optical object sensors of the same side are connected in parallel to form a sensor group. Each sensor group (Side A and Side B) are powered with different voltage level (24V to 12V and 12V to 0V) to give three possible output levels (24V, 12V and 0V) for three possible scenarios: no object,

object at Side A and object at Side B. The output from these sensors are fed into the other channel of the oscilloscope as a trigger or reference signal. The physical setup of the experiment is as shown in Fig. 15.



**Fig. 14. The setup of the optical object sensors**

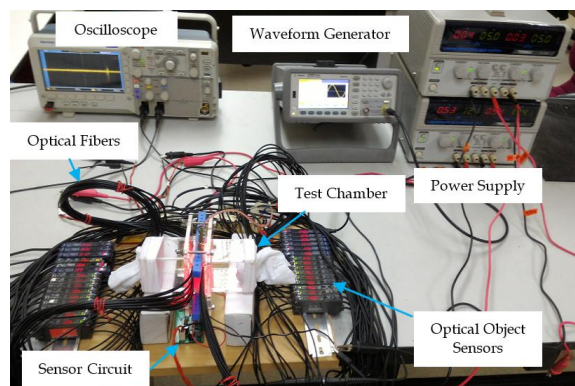


**Fig. 15. Experimental setup**

## V. RESULTS AND DISCUSSION

The experimental setup discussed in prior section is used on two medically important mosquito species: *Aedes albopictus* and *Culex quinquefasciatus*. *Aedes albopictus* are infamous for their role in transmitting dengue fever, Zika fever, yellow fever, and Chikungunya fever. Similar in importance, *Culex quinquefasciatus*, a common domestic mosquito is known for spreading encephalitis, Zika fever, filariasis and West Nile fever.

During the experiment, a single mosquito specimen is released into the test chamber and allowed to interact with the sensing electrodes. The male and female counterpart for each species is tested and recorded separately. Each experiment is repeated with 40 wild mosquitos (10 mosquitos per type) captured locally in domestic areas around Kota Kinabalu, Sabah.

### 5.1 Sensor Response

The results in this section are obtained from manual and careful observation on the location and movement of the sample in the test chamber, relative to the sensing electrodes. The oscilloscope is set to roll-mode at 400ms per division to actively display the waveform outputted from the capacitive sensor

circuit, while providing enough time for the experimenter to observe and react. Shown in Fig. 16 are the sensor output corresponding to the action, location and movement of a male *Aedes albopictus* captured on the oscilloscope.

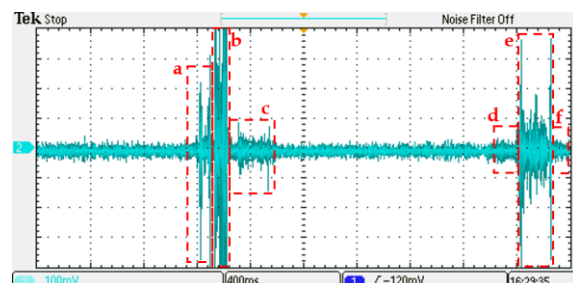


**Fig. 16. Sensor output for a male *Aedes albopictus***

By referring to the screenshot of the oscilloscope in Fig. 16, the labeled signal snippets are the results of the events illustrated in Fig. 17:

- a. the specimen zooms towards the sensing electrodes
- b. the specimen crosses the gap between the sensing electrodes
- c. the specimen departs and hovers away from the sensing electrodes
- d. the specimen approaches the sensing electrodes
- e. the specimen hovers near the sensing electrodes
- f. the specimen leaves the sensing electrodes without crossing the gap

From the result in this section, it is obvious that the proposed capacitive wing-beat sensor is able to capture the wing-beat signal of a flying mosquito for these following conditions:

1. slow approaching
2. slow leaving
3. hovering at one place
4. fast moving/darting
5. between the electrodes/grid.

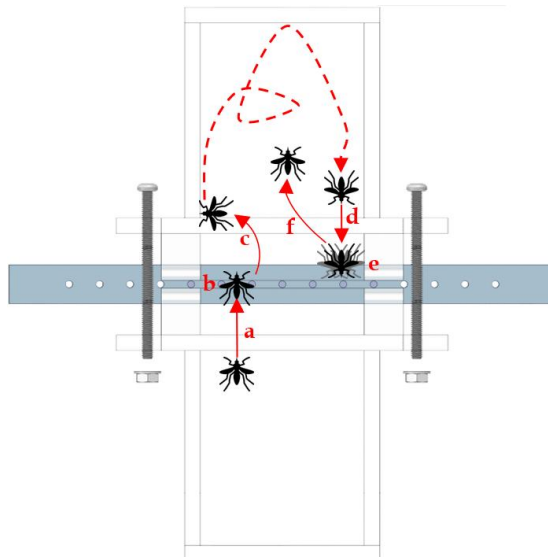


**Fig. 17. The events of the specimen viewed from the top of the test chamber**

### 5.1 Sensor Response

After the manual data collection in prior section, this section utilizes the optical object sensors to automate the recording of the capacitive sensor output. This is done by setting the oscilloscope to single-shot at 400ms per division and the output from the object sensors as the trigger. With this configuration, the oscilloscope will be triggered whenever the specimen enters the object sensors' view. The output from the capacitive sensor is recorded at 312,500 samples/s at 8-bit resolution in 4-second snippets. These recorded snippets are then processed individually to obtain the spectrogram.

By analyzing the spectrogram of the recorded male *Aedes albopictus* wing-beat in Fig. 18, the frequency components can be discerned clearly: fundamental frequency at 550Hz, second harmonic at 1100Hz and third harmonic at 1650Hz.

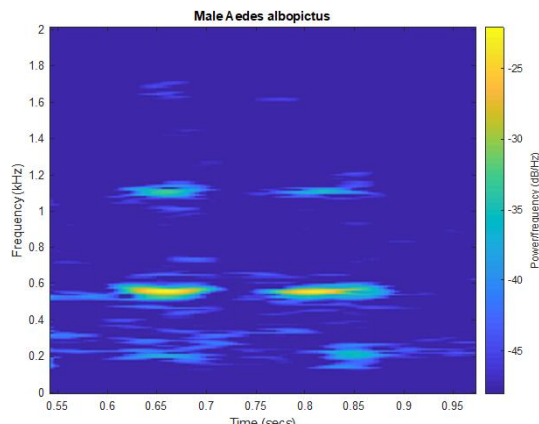


**Fig. 18. Wing-beat spectrogram of male *Aedes albopictus***

The spectrogram of the recorded female *Aedes albopictus* wing-beat in Fig. 19 shows the fundamental frequency at 460Hz and second harmonic at 920Hz.

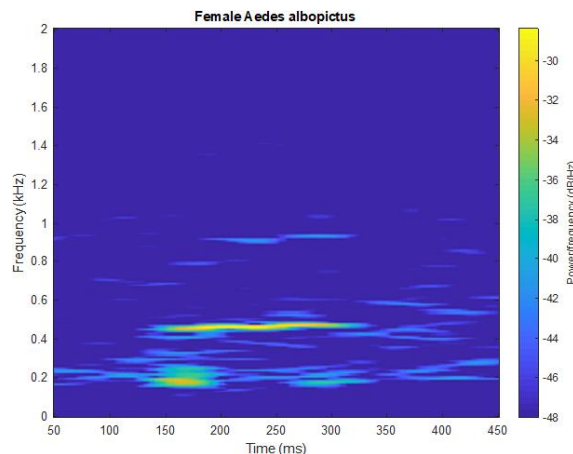


**Fig. 19. Wing-beat spectrogram of female *Aedes albopictus***

Shown in Fig. 20 is the spectrogram of the recorded male *Culex quinquefasciatus* wing-beat signal. The observed fundamental and second harmonic components are 750Hz and 1520Hz respectively.

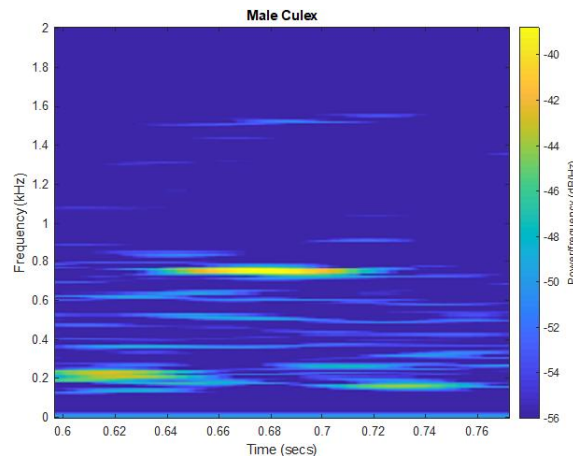


**Fig. 20. Wing-beat spectrogram of male *Culex quinquefasciatus***

As for the female *Culex quinquefasciatus*, the fundamental frequency and second harmonic of the recorded wing-beat signal are determined in Fig. 21 as 440Hz and 880Hz respectively.

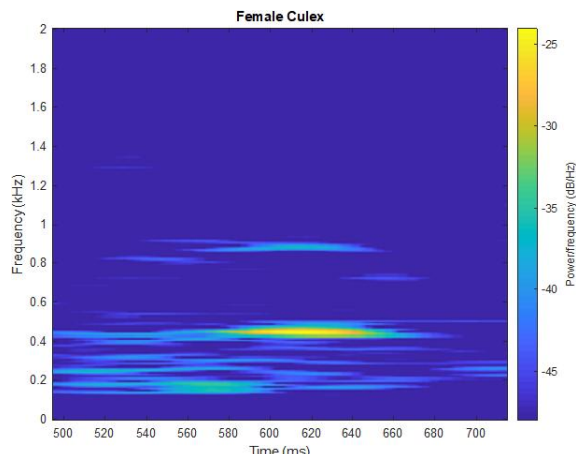


**Fig. 21. Wing-beat spectrogram of female *Culex quinquefasciatus***

It is observed that the third and higher harmonics of the wing-beat signals in the spectrograms are absent for both male and female *Culex quinquefasciatus* as well as female *Aedes albopictus*. This is caused by the limited resolution of the recorded samples, since the oscilloscope employed in this paper has a maximum vertical resolution of only 8-bit.

## VI. CONCLUSION

This paper has proposed the possibility of creating a low-cost and robust intelligent mosquito trap by integrating a capacitive wing-beat sensor into current commercial insect electrocuting traps. This core idea is explored in this paper by developing a preliminary capacitive sensor for detecting mosquito wing-beat. With the electrodes of the proposed capacitive sensor mimicking the electrocuting grids of commercial electric insect trap, the sensor is shown to be capable of detecting the wing-beat of common vector mosquitos (*Culex quinquefasciatus* and *Aedes albopictus*) at different airborne position and movement when tested in a controlled environment. The initial results of this paper highlight a promising direction and a possibility for actually implementing the sensor in intelligent traps.

## REFERENCES

- [1] WHO, *World Malaria Report 2018*. Luxembourg: WHO, 2018.
- [2] Z. Jamil, Y. Waheed, and T. Z. Durrani, "Zika virus, a pathway to new challenges," *Asian Pac. J. Trop. Med.*, vol. 9, no. 7, pp. 626–629, 2016, doi: 10.1016/j.apjtm.2016.05.020.
- [3] M. Geier *et al.*, "The BG-Counter: A smart Internet of Things (IoT) device for monitoring mosquito trap counts in the field while drinking coffee at your desk.," *Biogents*, no. February, pp. 1–2, 2016.
- [4] J. Medlock, T. Balenghien, B. Alten, V. Versteirt, and F. Schaffner, "Field sampling methods for mosquitoes, sandflies, biting midges and ticks," 2018. doi: 10.2903/sp.efsa.2018.EN-1435.
- [5] H. Mukundarajan, F. J. H. Hol, E. A. Castillo, C. Newby, and M. Prakash, "Using mobile phones as acoustic sensors for high-throughput mosquito surveillance," *Elife*, vol. 6, p. e27854, 2017, doi: 10.1101/120519.
- [6] D. G. Vasconcelos, "Biodiversity monitoring using smart acoustic sensors: application to mosquitos," University of Madeira, 2017.
- [7] I. Potamitis and I. Rigakis, "Novel Noise-Robust Optoacoustic Sensors to Identify Insects Through Wingbeats," *IEEE Sens. J.*, vol. 15, no. 8, pp. 4621–4631, 2015, doi: 10.1109/JSEN.2015.2424924.
- [8] I. Potamitis, I. Rigakis, and N. A. Tatlas, "Automated surveillance of fruit flies," *Sensors*, vol. 17, no. 1, p. 110, 2017, doi: 10.3390/s17010110.
- [9] I. Potamitis, I. Rigakis, N. Vidakis, M. Petousis, and M. Weber, "Affordable Bimodal Optical Sensors to Spread the Use of Automated Insect Monitoring," *J. Sensors*, vol. 2018, pp. 1–25, 2018, doi: 10.1155/2018/3949415.
- [10] I. Rigakis, I. Potamitis, N.-A. Tatlas, I. Livadaras, and S. Ntalampiras, "A Multispectral Backscattered Light Recorder of Insects' Wingbeats," *Electronics*, vol. 8, no. 3, p. 277, 2019, doi: 10.3390/electronics8030277.
- [11] I. R. Richards, "Photoelectric Cell Observations of Insects in Flight," *Nature*, vol. 175, p. 128, Jan. 1955, [Online]. Available: <http://dx.doi.org/10.1038/175128b0>.
- [12] K. Li and J. C. Principe, "Automatic Insect Recognition Using Optical Flight Dynamics Modeled By Kernel Adaptive Arma Network," in *2017 IEEE International Conference on Acoustics, Speech and Signal Processing (ICASSP)*, 2017, pp. 2726–2730, [Online]. Available: file:///D/Desktop/nevzat OLGUN 1. TİK/kaynaklar/deep learning/01\_Automatic insect recognition using optical flight dynamics modeled by kernel adaptive ARMA network2017.pdf.
- [13] E. R. Mullen, P. Rutschman, N. Pegram, J. M. Patt, J. J. Adamczyk, and Johanson, "Laser system for identification, tracking, and control of flying insects," *Opt. Express*, vol. 24, no. 11, p. 11828, 2016, doi: 10.1364/OE.24.011828.
- [14] I. Potamitis and I. Rigakis, "Large aperture

- optoelectronic devices to record and timestamp insects' Wingbeats," *IEEE Sens. J.*, vol. 16, no. 15, pp. 6053–6061, 2016, doi: 10.1109/JSEN.2016.2574762.
- [15] T. H. Ouyang, E. C. Yang, J. A. Jiang, and T. Te Lin, "Mosquito vector monitoring system based on optical wingbeat classification," *Comput. Electron. Agric.*, vol. 118, pp. 47–55, 2015, doi: 10.1016/j.compag.2015.08.021.
- [16] Y. Chen, "Mining Time Series Data: Flying Insect Classification and Detection," University of California Riverside, 2015.
- [17] Y. Chen, A. Why, G. Batista, A. Mafrá-Neto, and E. Keogh, "Flying Insect Classification with Inexpensive Sensors," *J. Insect Behav.*, vol. 27, no. 5, pp. 657–677, 2014, doi: 10.1007/s10905-014-9454-4.
- [18] S. A. A. Rahuman, J. Veerappan, R. V. Rajesh, S. A. A. Rahuman, J. Veerappan, and R. V. Rajesh, "Classification of Flying Insects with high performance using improved DTW algorithm based on hidden Markov model," *Brazilian Arch. Biol. Technol.*, vol. 59, no. December, pp. 1–12, 2016, doi: 10.1590/1678-4324-2016161054.
- [19] D. F. Silva, V. M. A. De Souza, G. E. A. P. A. Batista, E. Keogh, and D. P. W. Ellis, "Applying machine learning and audio analysis techniques to insect recognition in intelligent traps," in *Proceedings - 2013 12th International Conference on Machine Learning and Applications, ICMLA 2013*, 2013, vol. 1, pp. 99–104, doi: 10.1109/ICMLA.2013.24.
- [20] Y. Qi, G. T. Cinar, V. M. A. Souza, G. E. A. P. A. Batista, Y. Wang, and J. C. Principe, "Effective insect recognition using a stacked autoencoder with maximum correntropy criterion," *Proc. Int. Jt. Conf. Neural Networks*, vol. 2015-Septe, 2015, doi: 10.1109/IJCNN.2015.7280418.
- [21] A. Ching, E. Jackson, M. J. Sinclair, and P. Therien, "Insect trap," US20170354135A1, 2017.
- [22] S. Majambere, D. J. Massue, Y. Mlacha, N. J. Govella, S. M. Magesa, and G. F. Killeen, "Advantages and limitations of commercially available electrocuting grids for studying mosquito behaviour," *Parasites and Vectors*, vol. 6, no. 1, p. 1, 2013, doi: 10.1186/1756-3305-6-53.
- [23] S. Dugassa, J. M. Lindh, S. W. Lindsay, and U. Fillinger, "Field evaluation of two novel sampling devices for collecting wild oviposition site seeking malaria vector mosquitoes: OviART gravid traps and squares of electrocuting nets," *Parasites and Vectors*, vol. 9, no. 1, pp. 1–11, 2016, doi: 10.1186/s13071-016-1557-7.
- [24] A. Braun, R. Wichert, A. Kuijper, and D. W. Fellner, "Capacitive proximity sensing in smart environments," *J. Ambient Intell. Smart Environ.*, vol. 7, no. 4, pp. 483–510, 2015, doi: 10.3233/AIS-150324.
- [25] R. Sobot, *Wireless Communication Electronics: Introduction to RF Circuits and Design Techniques*. London, Canada: Springer, 2012.
- [26] G. E. A. P. A. Batista, Y. Hao, E. Keogh, and A. Mafrá-Neto, "Towards automatic classification on flying insects using inexpensive sensors," *Proc. - 10th Int. Conf. Mach. Learn. Appl. ICMLA 2011*, vol. 1, pp. 364–369, 2011, doi: 10.1109/ICMLA.2011.145.